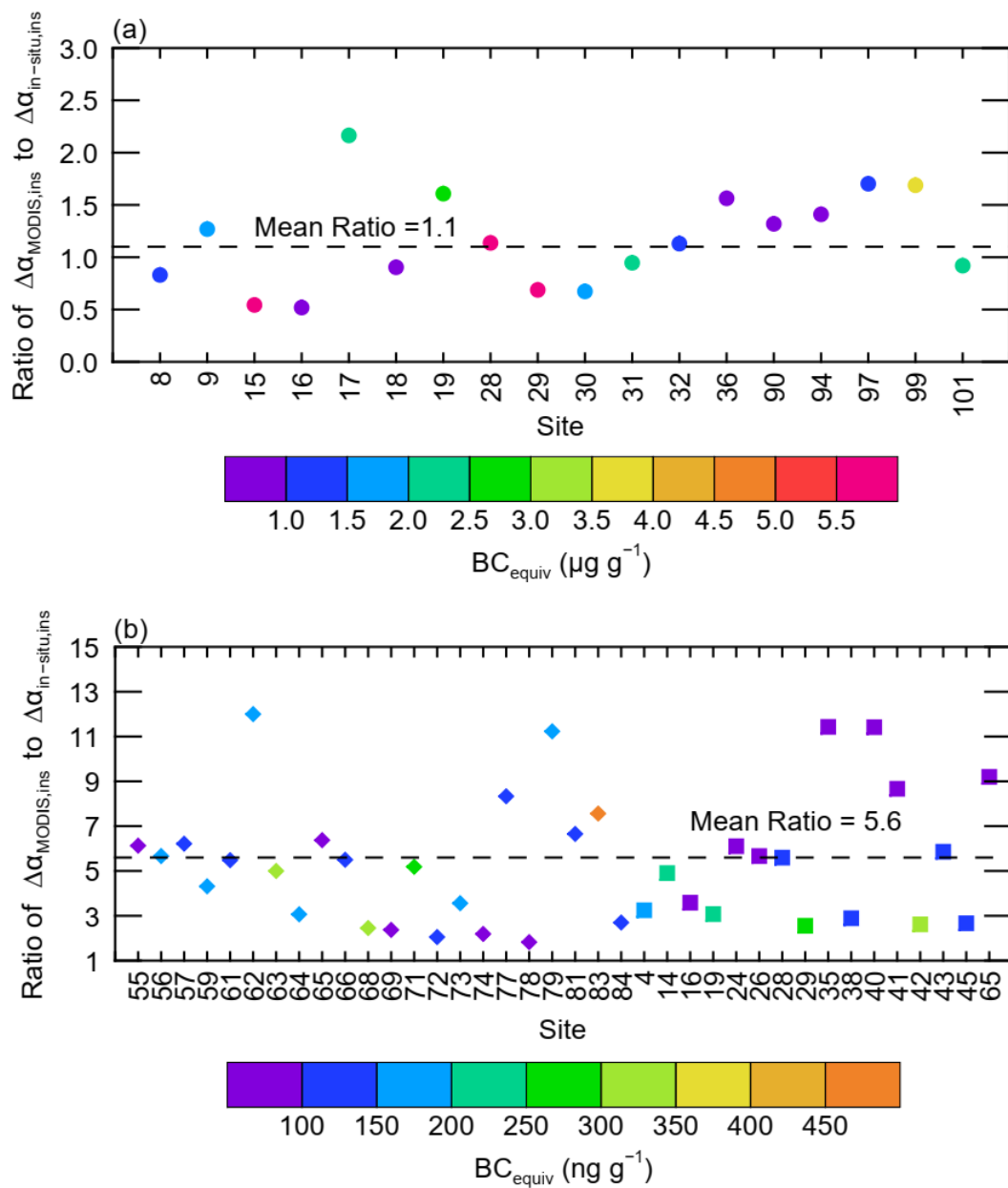1

2 **Figure S1.** (a) Average January–February incident direct solar spectra for latitudes 35°–75°, derived from the

3 SBDART model during clear-sky conditions. (b) Same as (a), but for diffuse solar irradiation.

Figure S2. Ratio of $\Delta\alpha_{MODIS,ins}$ to $\Delta\alpha_{in-situ,ins}$ for (a) heavily and (b) slightly polluted sites. Circles, diamonds, and squares represent the snow samples collected in NEC, NWC, and NA, respectively.
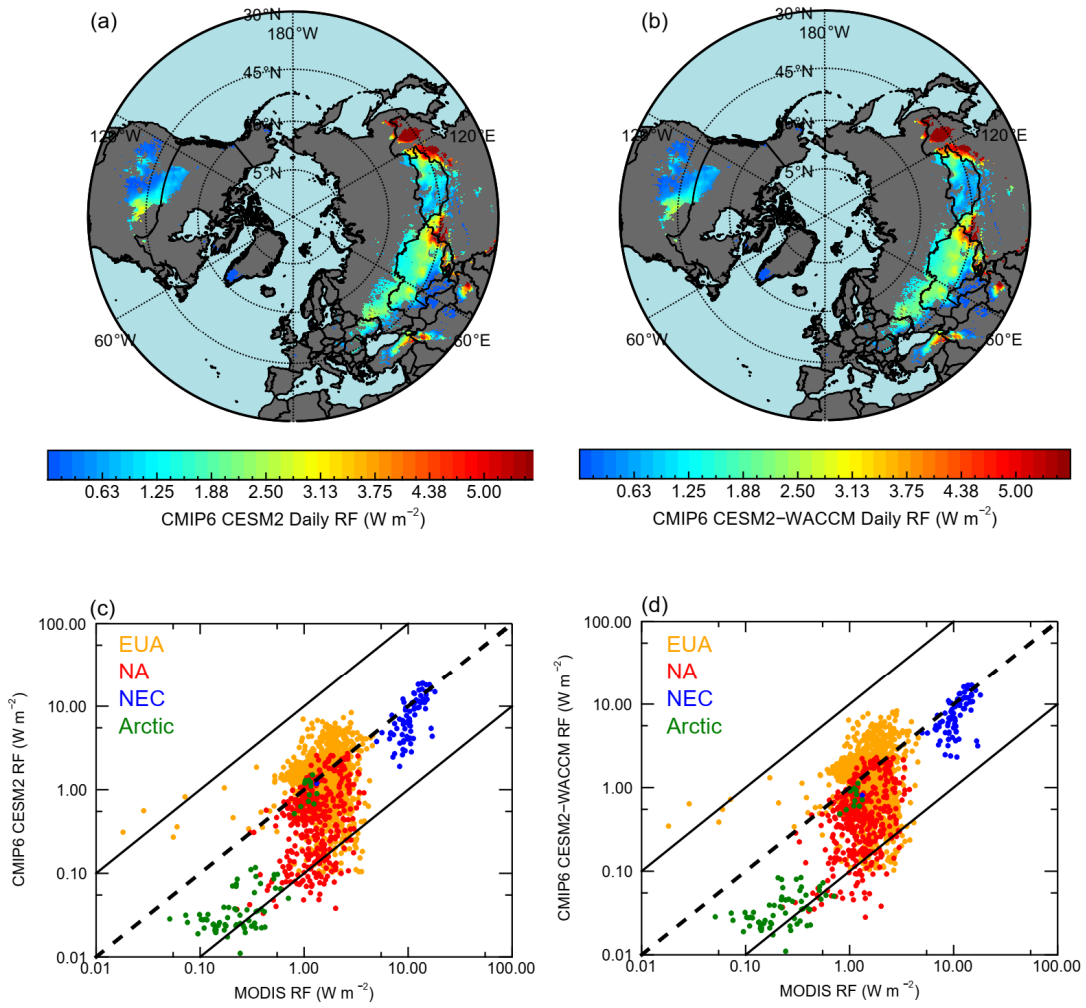
1

2
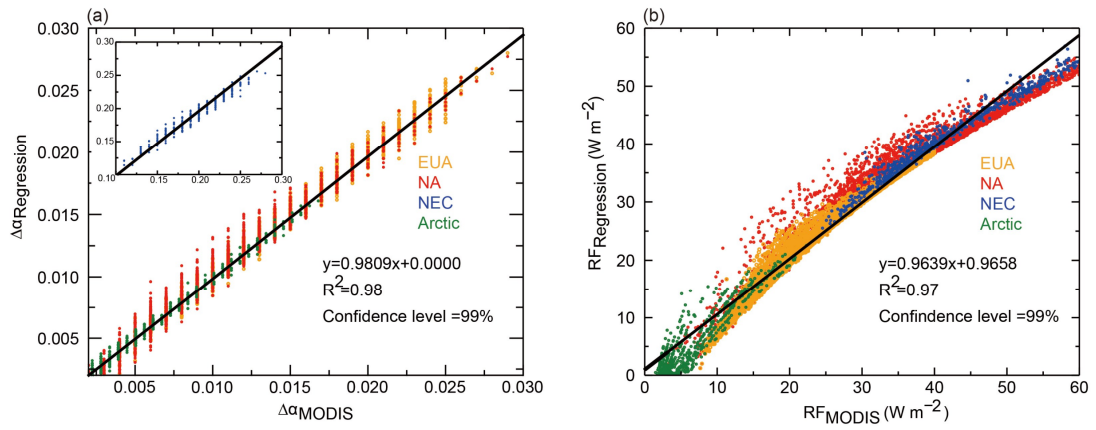
Figure S3. Comparisons of (a) $\Delta\alpha_{MODIS}$ and fitted albedo reduction ($\Delta\alpha_{Regression}$), and (b) RF_{MODIS} and fitted radiative forcing ($RF_{Regression}$). Different colors represent different regions.
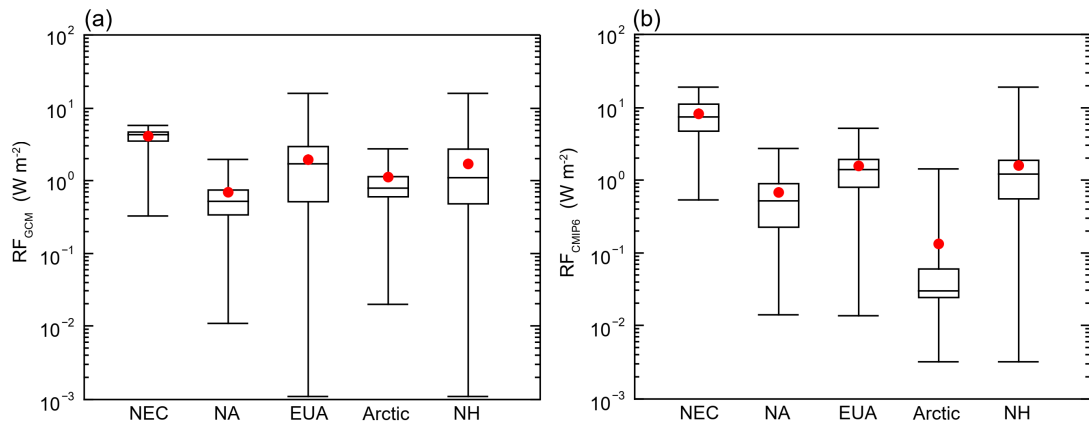
5

1

2

3 **Figure S4.** Spatial distributions of daily radiative forcing based on the soot content of snow from (a) CESM2
4 WACCM and (b) CESM2 in January–February for the period 2003–2014. Scatterplots of MODIS-retrieved daily
5 radiative forcing versus those of (c) CESM2-WACCM and (d) CESM2, respectively.

6

1

Figure S5. Statistics of (a) springtime radiative forcing due to LAPs in the Northern Hemisphere snowpack, from the GCM run of Flanner et al. (2009), and (b) daily radiative forcing, based on the CMIP6 soot content of snow in January–February during the period 2003–2014. The boxes denote the 25th and 75th quantiles, and the horizontal lines represent the 50th quantiles (medians), the averages are shown as red dots; the whiskers denote the 5th and 95th quantiles.